AIAA JOURNAL
Vol. 46, No. 9, September 2008

Material Uncertainty Propagation in Helicopter Nonlinear Aeroelastic Response and Vibration Analysis

Senthil Murugan,* Dineshkumar Harursampath,† and Ranjan Ganguli‡
Indian Institute of Science, Bangalore 560 012, India

DOI: 10.2514/1.35941

The effect of uncertainty in composite material properties on the nonlinear aeroelastic response and vibratory loads of a four-bladed composite helicopter rotor is studied. The aeroelastic analysis is done using a finite element method in space and time, and the composite cross section is analyzed using a variational asymptotic approach. The effective material properties of composite laminas are first considered as random variables with a coefficient of variation of 5%. The material uncertainty is propagated to cross-sectional stiffness, rotating natural frequencies, aeroelastic response, and vibratory loads of the composite helicopter rotor. The stochastic cross-sectional and aeroelastic analyses are carried out with Monte Carlo simulations. The stochastic stiffness values are scattered up to 15% around the baseline stiffness values and show a Gaussian distribution with a coefficient of variation of about 4%. The uncertainty impact on rotating natural frequencies depends on the level of centrifugal stiffening for different modes. The stochastic rotating natural frequencies indicate a possibility of their coincidence with the integer multiples of rotor speed. The propagation of material uncertainty into aeroelastic response causes large deviations from the baseline predictions and affects the crucial higher harmonics content, which is critical for vibration predictions. The magnitudes of 4/rev vibratory loads show a scattering up to 300% from the baseline value, and their probability density functions show non-Gaussian-type distributions. Further, the uncertainty results for a coefficient of variation of 10% in the material properties are obtained. The uncertainty impact on the aeroelastic response is found to be proportional to the coefficient of variation of the composite material properties.

I. Introduction

THE highly multidisciplinary and complex nature of rotorcraft aeroelasticity has led researchers to focus on improving the fidelity of analytical modeling, developing new solution methods, and validating the aeroelastic results with experimental or flight test data [1–4]. With these advances in computational methods, the predicted aeroelastic performance can still deviate from the actual system response because of the randomness associated with the parameters and operating conditions defined for an aeroelastic analysis. In recent years, much interest has focused on incorporating uncertainties into the aeroelastic analysis [5]. When compared with the research on fixed-wing aircraft [6–10], very few studies have focused on the uncertainty issues involved in rotorcraft aeroelastic analysis and quantification of these uncertainties on its response [11]. However, uncertainty quantification is a key issue in aeroelasticity [5].

Uncertainties can generally be classified as aleatory (random) and epistemic (subjective)[12]. Aleatory uncertainties can be defined as the inherent variations associated with the system parameters or the environment under consideration and are also referred as variabilities, irreducible uncertainties, inherent uncertainties, and stochastic uncertainties. Aleatory uncertainties are generally modeled using a probabilistic description. In structural mechanics, the randomness in mechanical properties such as mass, stiffness, and geometrical imperfections because of fabrication errors or lack of quality controls can be classified as aleatory uncertainties. In the context of aeroelasticity, in addition to structural uncertainty, the randomness in parameters such as wind velocity, lift, and drag coefficients can also be termed as aleatory uncertainties [13,14].

On the other hand, epistemic uncertainty derives from a lack of knowledge or information in any phase of the modeling process and little or no experimental data for a physical parameter. It is also termed as reducible uncertainty, subjective uncertainty, and model-form uncertainty. In structural mechanics, the ignorance of material or geometrical nonlinearity and exclusion of shear deformation in analytical models, definition of failure for a structure, and lack of accurate information about structural damping can be termed as epistemic uncertainties. In aeroelasticity, which is a multiphysics problem, lack of high-fidelity aerodynamic models or unmodeled nonclassical or nonlinear structural effects can be categorized as epistemic. Therefore, a better understanding of the physical process or availability of sufficient data can curtail the epistemic uncertainty of the system. Most current work on rotorcraft aeroelasticity focuses on improved modeling and therefore addresses the reduction of epistemic uncertainty. Corresponding research toward quantifying and reducing the adverse effects of aleatory uncertainty are very limited [11].

Rotorcraft aeroservoelasticity couples the fluid, structure, and control domains. The randomness in the input parameters (aleatory) and the fidelity of mathematical models for analysis (epistemic) in each domain can influence the predicted response. From the structural perspective, composite materials, which are extensively used in today's rotor blades, are a major source of aleatory uncertainty. The macrolevel material properties of a composite lamina depend on the microlevel properties such as fiber and matrix material properties and fabrication variables such as fiber volume ratio, misalignment of fibers leading to fluctuations in ply-angle orientation, variation in ply thickness, fiber waviness or undulation, intralamina voids, incomplete curing of resin, and excess resin between plies. These variables are statistical in nature and influence the macrolevel mechanical properties of composite lamina [15–20]. Therefore, the effect of randomness (aleatory) in composite mechanical properties on rotorcraft aeroelasticity should be evaluated. Such uncertainties can affect the interpretation of results in which aeroelastic analysis results are compared with the experimental or flight test data [3,4].

Presented as Paper 2298 at the 48th AIAA/ASME/ASCE/AHS/ASC Structures, Structural Dynamics, and Materials Conference, Honolulu, HI, 23–26 April 2007; received 30 November 2007; revision received 29 May 2008; accepted for publication 29 May 2008.

*Graduate Student, Department of Aerospace Engineering; murga@aero.iisc.ernet.in. Member AIAA.
†Assistant Professor; dinesh@aero.iisc.ernet.in. Senior Member AIAA.
‡Associate Professor; ganguli@aero.iisc.ernet.in. Senior Member AIAA.

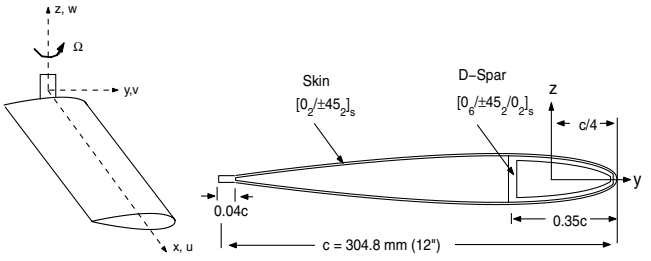

Fig. 1 Details of the rotor blade and its cross section.

The fidelity of a mathematical model for composite-blade cross-sectional analysis is also a source of uncertainty (epistemic) other than the randomness in material properties. Most works on composite rotor blades have used analytical models for cross-sectional analysis [21–24]. The analytical models have restrictions on the complexity of blade cross section when compared with the detailed finite element analysis. A finite element method based on variational asymptotic beam sectional (VABS) analysis can handle complicated airfoil cross sections and structural inhomogeneity of a realistic helicopter rotor blade [25,26]. Such an analysis can also accurately capture important nonclassical and nonlinear effects present in composite rotating beams and thereby reduce epistemic uncertainty.

Several stochastic methods are available for uncertainty analysis [27–33]. These methods can generally be categorized as intrusive and nonintrusive methods from a computational perspective. The intrusive methods need the governing equations and deterministic analysis programs to be modified to perform uncertainty analysis. In the nonintrusive methods, uncertainty analysis can be performed without any modification of the governing equations or the analysis programs. Monte Carlo simulations (MCS) constitute the most popular nonintrusive uncertainty-analysis technique.

In this study, the material properties of composite laminas used in the rotor blades are considered as random variables. The impact of these material uncertainties on the rotor aeroelastic response and vibratory loads are studied. The uncertainty analysis is performed using the direct MCS. The primary reasons for selecting MCS are as follows:

1) The rotorcraft aeroelastic codes are complex in nature and need domain experts for incorporating any intrusive uncertainty-analysis technique.

2) The advanced computing machines available currently consume less computational time for each rotorcraft aeroelastic simulation, making MCS practically feasible [34].

The material uncertainty is first propagated to the cross-sectional stiffness of the rotor blade. From the cross-sectional stiffness, uncertainty is propagated to rotating natural frequencies, nonlinear aeroelastic response, and vibratory loads of the helicopter rotor blade.

Table 1 Helicopter properties

Number of blades	4
Radius R, m	4.94
Rotor angular speed Ω, rad/s	40.12
Mass m, kg/m	6.46
Solidity σ	0.10
C_T/σ	0.07
Lock number γ	6.34

Table 2 Material properties of graphite/epoxy

Property	Mean
E_1, GPa	141.96
E_2, E_3, GPa	9.79
G_{12}, G_{13}, GPa	6.00
G_{23}, GPa	4.80
ν_{12}, ν_{13}	0.30
ν_{23}	0.34

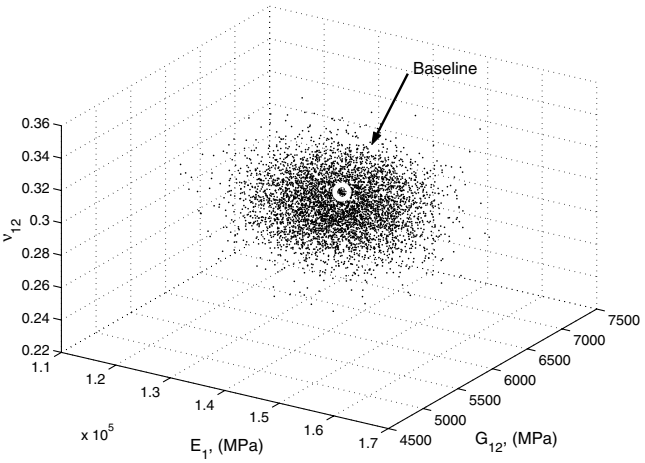

Fig. 2 Monte Carlo simulation results of composite material properties.

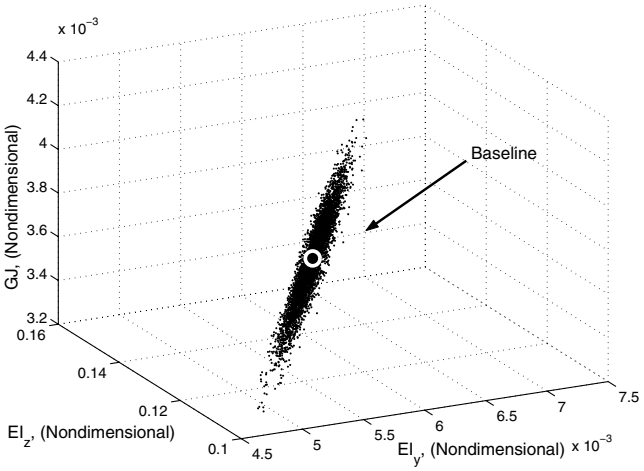

Fig. 3 Monte Carlo simulation results of rotor blade stiffness.

II. Rotor Blade Cross-Sectional Analysis

A critical aspect of helicopter rotor dynamic analysis is the calculation of equivalent 1-D beam properties for the 3-D rotor blade. The VABS analysis provides the 1-D beam properties of composite blades accurately and is computationally efficient [25]. In the variational asymptotic procedure, the 3-D strain field is expressed in terms of 1-D strain measures and unknown cross-sectional warping functions (which account for the cross-sectional out-of-plane and cross-sectional in-plane deformations). The strain energy density of the beam is then minimized to determine the warping functions in terms of 1-D strain measures. The warping functions are determined asymptotically based on the orders of the small parameters involved. Based on such an analysis, the classical stiffness model of a rotor blade turns out to be the most rudimentary, yet asymptotically

Table 3 Statistics of cross-sectional stiffness

Stiffness	Baseline	COV, %	
		Case I	Case II
$EA/m_o\Omega^2R^2$	523.43	4.47	8.95
$GJ/m_o\Omega^2R^4$	0.0037	3.42	6.88
$EI_y/m_o\Omega^2R^4$	0.0057	4.46	8.93
$EI_z/m_o\Omega^2R^4$	0.1249	4.21	8.44
$K_{14}/m_o\Omega^2R^3$	−2.2597	3.94	7.93

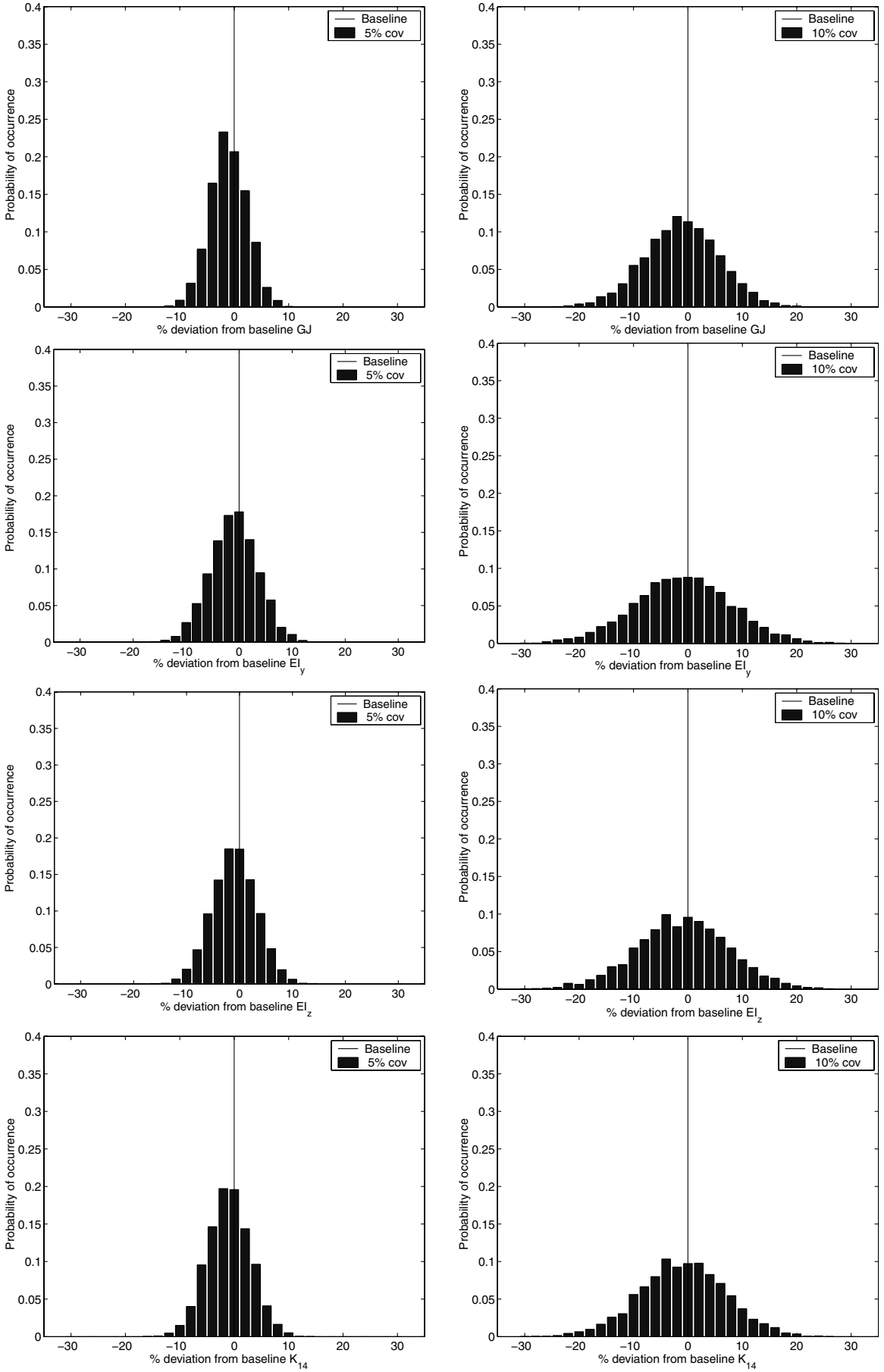

Fig. 4 Probability histograms of rotor blade cross-sectional stiffness.

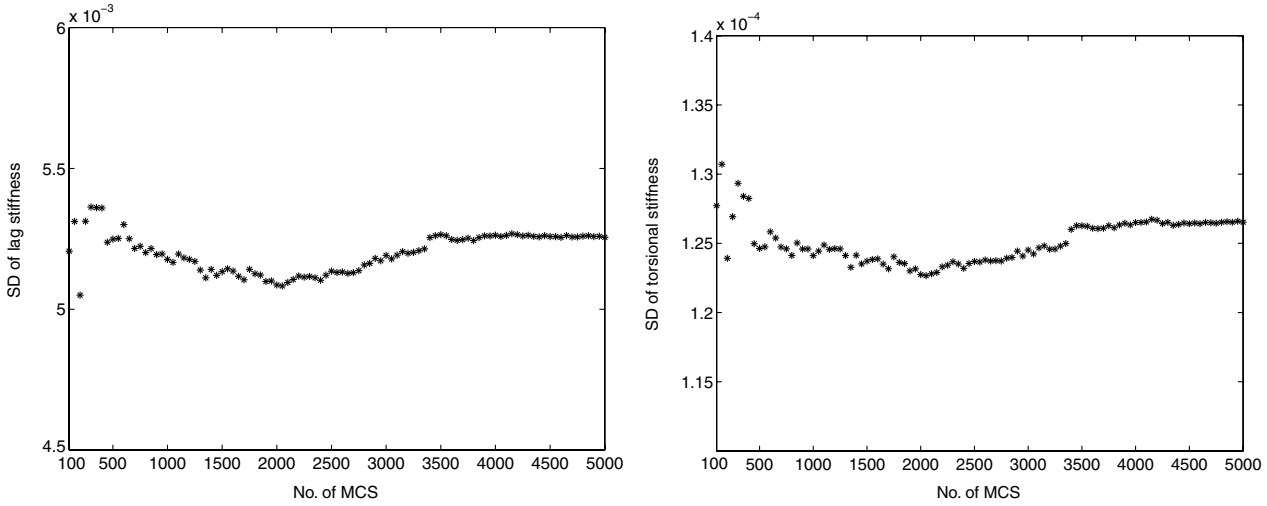

Fig. 5 Convergence of the lag and torsion stiffness.

correct, result and can be expressed as follows:

$$\begin{Bmatrix} F_x \\ M_x \\ -M_y \\ M_z \end{Bmatrix} = \begin{bmatrix} EA & K_{12} & K_{13} & K_{14} \\ K_{12} & GJ & K_{23} & K_{24} \\ K_{13} & K_{23} & EI_y & K_{34} \\ K_{14} & K_{24} & K_{34} & EI_z \end{bmatrix} \begin{Bmatrix} u' \\ \phi' \\ w'' \\ v'' \end{Bmatrix} \tag{1}$$

where u, v, and w, correspond to axial, lag (rotor in-plane), and flap (rotor out-of-plane) displacements, respectively, and ϕ corresponds to torsional displacement of the rotor blade, as shown in Fig. 1. The detailed formulation and the asymptotic procedure for cross-sectional analyses are given in [25].

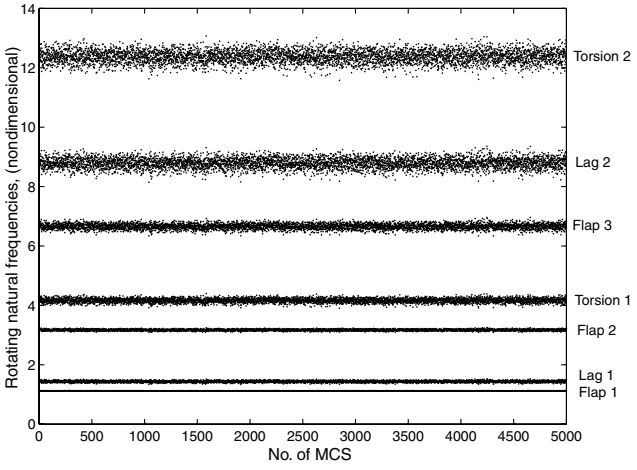

Fig. 6 Monte Carlo simulations of the rotating natural frequencies.

III. Nonlinear Aeroelastic Model

A comprehensive aeroelastic analysis code based on the finite element method in space and time is used to evaluate the helicopter blade response [35]. The helicopter is modeled as a nonlinear representation of composite rotor blades coupled to a rigid fuselage with 6 degrees of freedom. The rotor blade is modeled as a slender elastic beam undergoing flap bending displacement w, lag bending displacement v, elastic twist ϕ, and axial deflection u with a rotational speed of Ω, as shown in Fig. 1. The effect of moderate deflections is included by retaining second-order nonlinear terms. For a given blade, the governing equations are derived using a generalized Hamilton's principle, applicable to nonconservative systems:

$$\int_{\psi_1}^{\psi_2} (\delta U - \delta T - \delta W)\, \mathrm{d}\psi = 0 \tag{2}$$

where δU is the virtual strain energy, δT is the virtual kinetic energy of the elastic blade, δW is the virtual work done by the external aerodynamic forces acting on the blade, and $\psi = \Omega t$ is the azimuth angle of the blade around the rotor disk. The unsteady aerodynamics and free-wake models are used to calculate the aerodynamic forces [35]. The blade is discretized into beam finite elements, each with 15 degrees of freedom (DOF). These DOF correspond to 6 DOF $(u, v, v', w, w', \widehat{\phi})$ at each boundary node and two axial DOF (u) and

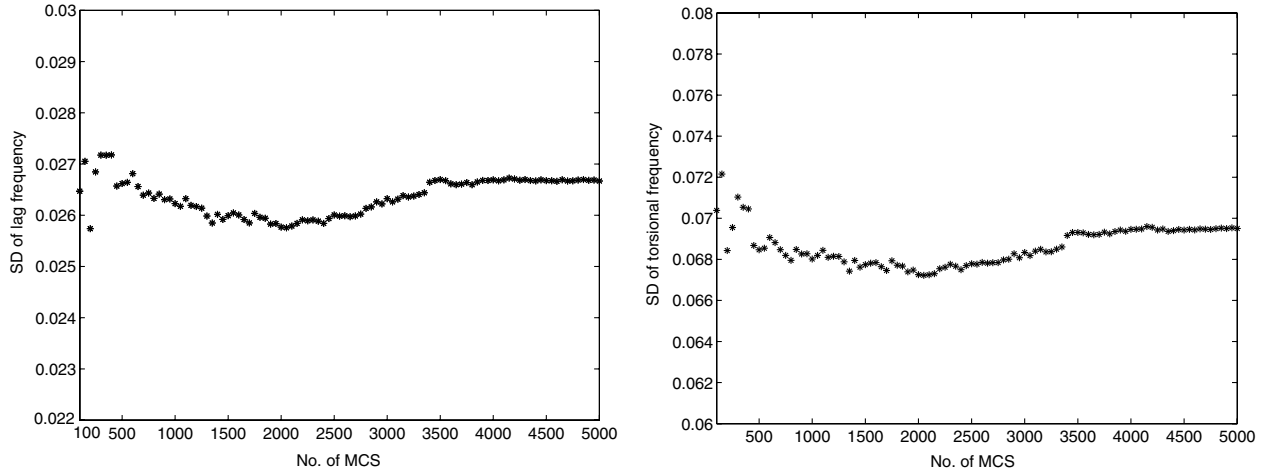

Fig. 7 Convergence of the lag and torsion rotating frequencies.

Table 4 Statistics of rotating natural frequencies

Mode	Baseline (per rev)	COV, %	
		Case I	Case II
Lag 1	1.44	1.85	3.73
Lag 2	8.79	1.94	3.92
Flap 1	1.12	0.21	0.42
Flap 2	3.17	0.73	1.47
Flap 3	6.65	1.31	2.63
Torsion 1	4.17	1.66	3.37
Torsion 2	12.38	1.70	3.44

one elastic twist ($\widehat{\phi}$) at internal nodes of the beam element. These DOF capture the cubic variations in axial and bending (flap and lag) deflections and quadratic variation in elastic torsion. The finite element equations are reduced in size by the normal mode transformation. This results in the nonlinear ordinary differential equation with periodic coefficients, as given next:

$$\mathbf{M}\,\ddot{\mathbf{p}}(\psi) + \mathbf{C}(\psi)\dot{\mathbf{p}}(\psi) + \mathbf{K}(\psi)\mathbf{p}(\psi) = \mathbf{F}(\mathbf{p}, \dot{\mathbf{p}}, \psi) \tag{3}$$

where **M**, **C**, **K**, **F**, and **p** represents the finite element mass matrix, damping matrix, structural stiffness matrix, finite element force vector, and modal displacement vector, respectively. Nonlinearities in the model occur primarily due to Coriolis terms and due to allowing of moderate deflection in the strain-displacement relations and nonuniform inflow. The preceding equations govern the dynamics of the rotor blade. These equations are then solved using a finite element in time in combination with the Newton-Raphson method. The solutions to the equations are then used to calculate rotor blade loads using the force summation method, in which aerodynamic forces are added to the inertial forces. The blade loads

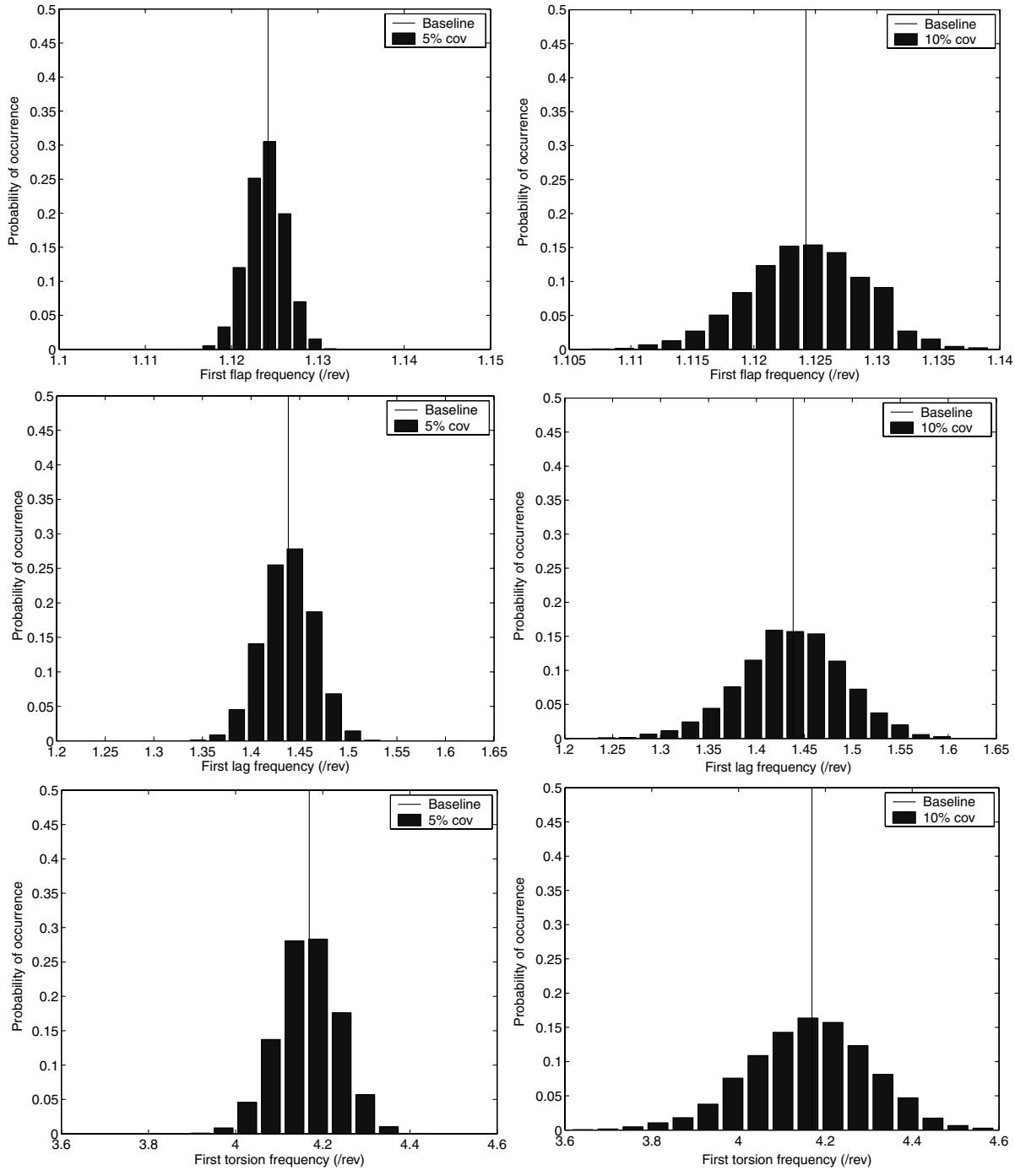

Fig. 8 Probability histograms of the fundamental rotating frequencies.

are integrated over the blade length and transformed to the fixed frame to get hub loads. The steady hub loads are used to obtain the forces acting on the rotor and combined with fuselage and tail rotor forces to obtain the helicopter rotor trim equations:

$$\mathcal{F}(\Theta) = \mathbf{0} \tag{4}$$

These nonlinear trim equations are also solved using the Newton–Raphson method. The helicopter rotor trim equations and the blade response equations (3) and (4) are solved simultaneously to obtain the blade steady response and hub loads. This coupled trim procedure is important for capturing the aeroelastic interaction between the aerodynamic forces and the blade deformations. Further details of the analysis are available in [35].

IV. Numerical Results

In this section, the effect of material uncertainties on the cross-sectional stiffness, rotating natural frequencies, aeroelastic response, and vibratory hub loads of the composite rotor blade are studied. The vehicle properties of a hingeless helicopter rotor used in this study are given in Table 1 [36]. A NACA0015 airfoil section with a 304.8-mm (12-in.) chord is selected for this study [37]. The details of the airfoil section are given in Fig. 1. The skin and the D-spar are considered to be made of graphite/epoxy plies with the material properties given in Table 2 [38]. Each ply is 0.127 mm (0.005 in.) thick. The stacking sequences for the skin and D-spar are selected as $[0_2/\pm 45_2]_s$ and $[0_6/\pm 45_2/0_2]_s$, respectively, so that the rotating natural frequencies of the rotor blades represent a stiff in-plane rotor [36].

A. Blade Cross-Sectional Stiffness

First, the impact of material uncertainty on the blade cross-sectional stiffness is evaluated. A random input variable x_i with a normal distribution can be given as

$$x_i = \mu + \sigma_i r_i \tag{5}$$

where μ is the mean, σ_i is the standard deviation, and r_i is any random number generated from a Gaussian distribution with a mean of 0 and a standard deviation of 1. The scatter in the macrolevel effective elastic properties of composite lamina $(E_1, E_2, G_{12}, G_{13}, \nu_{12}, \nu_{23})$ with respect to randomness in microlevel variables has been reported in the literature [15,16]. Therefore, in this study, the macrolevel elastic properties of composite lamina given in Table 2 are considered as independent random variables. The uncertainty analysis is carried out for two cases: in case I, a coefficient of variation (COV $= \sigma/\mu$) of 5% is considered for each material property, and in case II, a COV of 10% is considered for each material property. A COV of 5% is typical of randomness of composite materials [18] and a COV of 10% is used to study the effect of doubling the uncertainty level on the stochastic aeroelastic response of the rotor. However, the results discussed are for case I, unless it is stated as case II.

The direct MCS based on a simple random sampling method is used in this study [30]. In this approach, a probability distribution type for the random variable is first selected. Then a sampling set from the distribution is generated. Finally, the simulations are conducted using the generated sampling set. The cross-sectional stiffnesses of rotor blade are evaluated for 5000 random samples of material properties. The finite element based VABS code requires the geometry of the 2-D blade cross section with the details of nodes, elements, ply material, and ply orientation angles. Therefore, a subroutine is developed to provide the necessary details of the rotor blade cross section. The rotor blade cross section shown in Fig. 1 is meshed and the baseline stiffnesses are evaluated with the mean values of material properties. For MCS of cross-sectional stiffness, only the material properties defined in the VABS input file are changed randomly within their respective distributions, and remeshing of the cross section is not needed.

The baseline (deterministic) and nondeterministic stiffness values are evaluated for the cross section with the origin defined at the quarter-chord of the airfoil. The MCS of composite material properties and rotor blade cross-sectional stiffnesses are shown in Figs. 2 and 3. For visualization, only three of the six random material properties (E_1, G_{12}, and ν_{12}) and three of the cross-sectional stiffness terms (EI_y, EI_z, and GJ) are shown in these figures. The stochastic

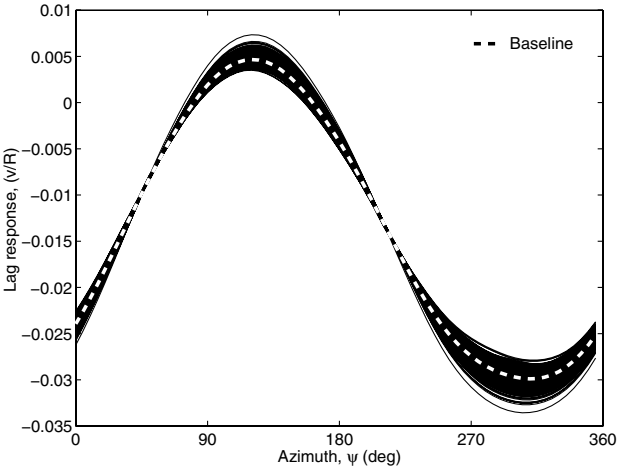

Fig. 9 Baseline and Monte Carlo simulation results for blade tip lag response.

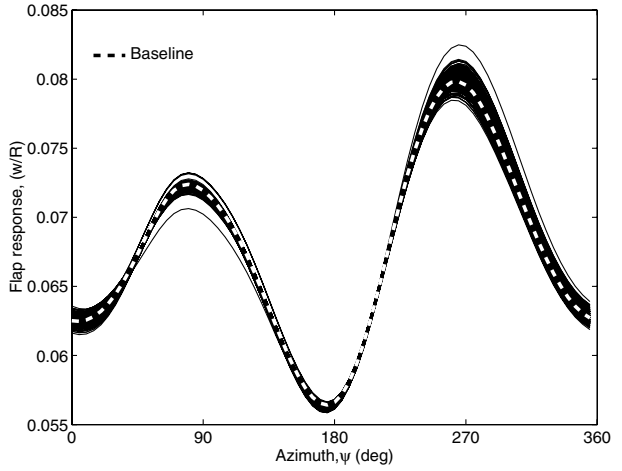

Fig. 10 Baseline and Monte Carlo simulation results for blade tip flap response.

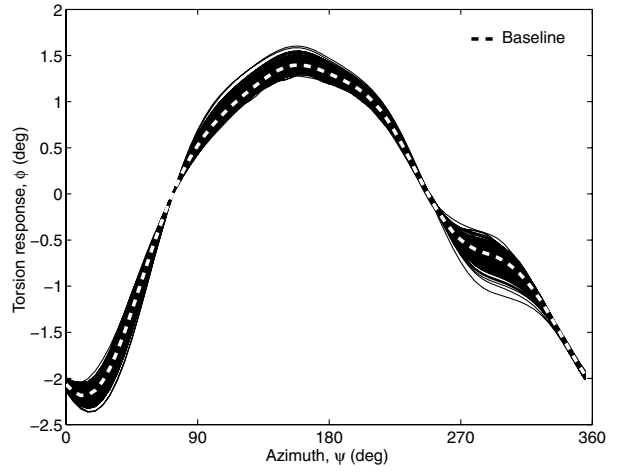

Fig. 11 Baseline and Monte Carlo simulation results for blade tip torsion response.

stiffness values are scattered up to ±15% around the baseline stiffness value. However, it is observed from Fig. 3 that the cross-sectional stiffnesses are not scattered throughout the design space, compared with the scatter in the material properties shown in Fig. 2. The baseline values and statistics of the cross-sectional stiffnesses are summarized in Table 3. The histograms of blade stiffnesses show normal distributions, as given in Fig. 4. Further, the increase in COV from 5 to 10% in material properties increases the spread of the probability distributions of stiffnesses while retaining their Gaussian nature. This can also be seen from the COV values given in Table 3, which show a proportional relationship between material property COV and stiffness COV.

The preceding results show that the aeroelastic analysis predictions with the baseline stiffness values have much less probability of remaining the same when material uncertainties are considered in the analysis. For the blade cross section considered, the elastic couplings other than the extension-lag coupling are very small. The extension-lag coupling stiffness also shows a normal distribution with 15% deviation around the baseline, as seen in Fig. 4. The adequacy of number of MCS is checked by the convergence of standard deviation of cross-sectional stiffness, as shown in Fig. 5. The 5000 MCS for stochastic cross-sectional analysis takes about 80 h of CPU time.

B. Rotating Natural Frequencies

The uncertainty impact on rotating natural frequencies of the rotor blade is studied with the stochastic stiffness values of the preceding

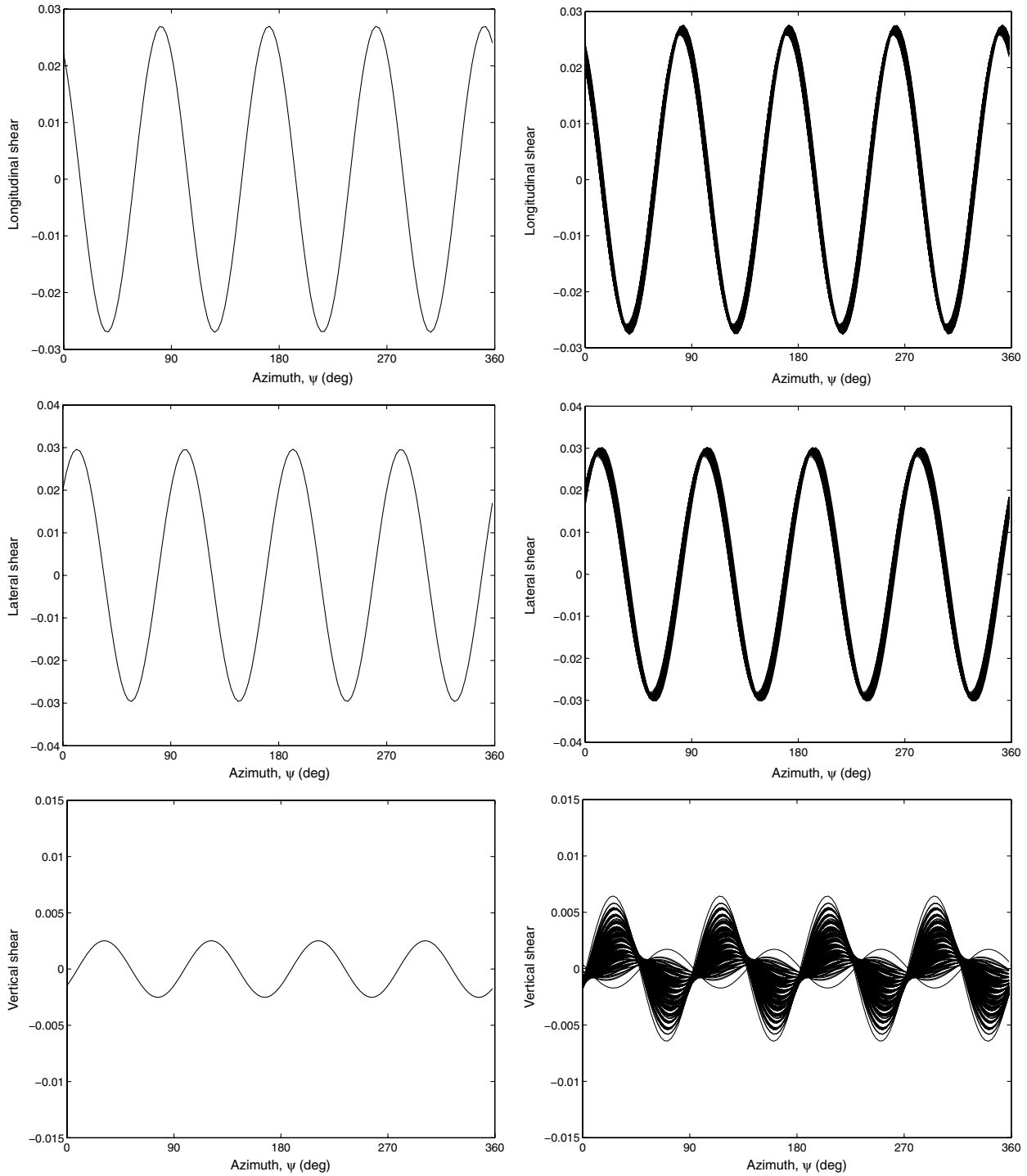

Fig. 12 Baseline and Monte Carlo simulation results for 4/rev vibratory hub loads (nondimensional).

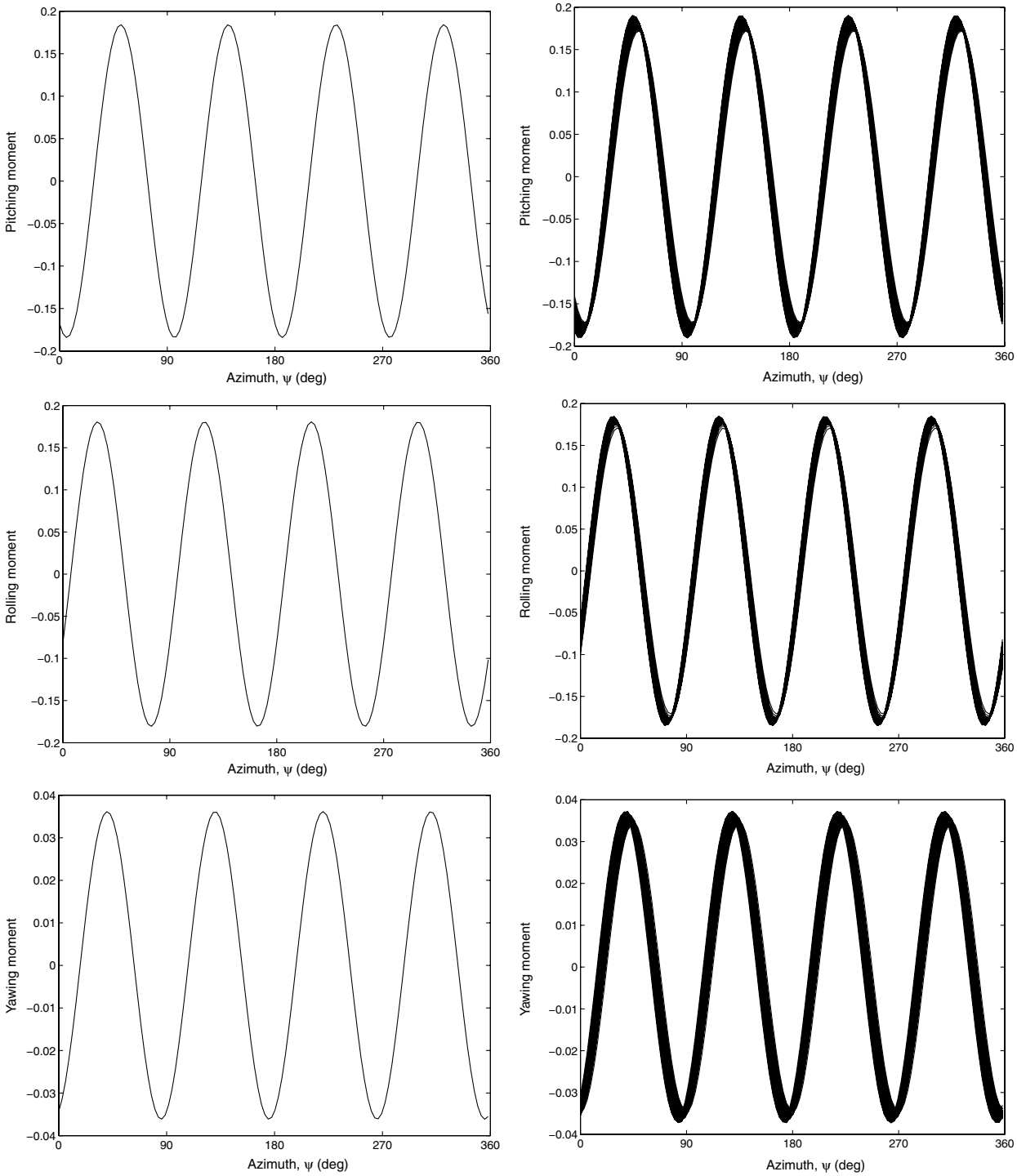

Fig. 13 Baseline and Monte Carlo simulation results for 4/rev vibratory moments (nondimensional).

section. The rotating natural frequencies are calculated by solving the following eigenvalue problem:

$$\mathbf{K}\,\Phi = \omega^2 \mathbf{M}\Phi \tag{6}$$

where the stiffness **K** includes the structural stiffness and centrifugal stiffening when the blade is rotating, **M** is the structural mass matrix, ω are the natural frequencies, and Φ contains the mode shapes.

Table 5 Uncertainty impact on the magnitude of 4/rev vibratory loads

Loads	Baseline	Mean	Median	Minimum (% deviation from baseline)	Maximum (% deviation from baseline)
F_x	0.0270	0.0269	0.0270	0.0250 (−7)	0.0283 (5)
F_y	0.0296	0.0295	0.0296	0.0276 (−7)	0.0303 (2)
F_z	0.0025	0.0027	0.0025	0.0005 (−82)	0.0100 (298)
M_x	−0.1806	−0.1803	−0.1806	−0.1880 (−8)	−0.1666 (4)
M_y	−0.1841	−0.1838	−0.1841	−0.1963 (−9)	−0.1671 (7)
M_z	−0.0361	−0.0361	−0.0361	−0.0419 (−7)	−0.0336 (16)

For the aeroelastic analysis, the first three normal modes for flap, two normal modes for lag, two for torsion, and one for axial motion are used to capture the essential dynamics of the system. The MCS of rotating natural frequencies of flap, lag, and torsion modes are shown in Fig. 6. The convergence of the MCS for the lag and torsion frequencies is shown in Fig. 7. It is observed that 5000 random samples are sufficient for the convergence of standard deviation of rotating natural frequencies. The baseline natural frequencies and their COVs for rotating blades are given in Table 4. The rotating blade shows a COV of 0.21, 1.85, and 1.66% for the fundamental flap, lag, and torsional frequencies, respectively. Thus, among the three fundamental frequencies, lag and torsion frequencies exhibit higher COVs, whereas the variation in flap frequency is comparatively less. However, the COVs of rotating natural frequencies increase for the higher modes of flap, lag, and torsion motions, as shown in Table 4. The histograms for flap, lag, and torsional fundamental frequencies of the rotating blade given in Fig. 8 show Gaussian distributions. Again, the effect of doubling the COVs in the material properties causes a proportional increase in the distributions. This can also be seen from the COVs shown in Table 4.

From Table 4, it is observed that the uncertainty impact on rotating natural frequencies varies for the flap, lag, and torsion modes. This is can be explained as follows. As is well known, in a rotating blade, the centrifugal stiffness (which is proportional to the rotational speed, blade mass, and blade length) plays a role in dynamics, in addition to the structural stiffness [39]. However, the uncertainty in elastic properties is propagated only to the structural

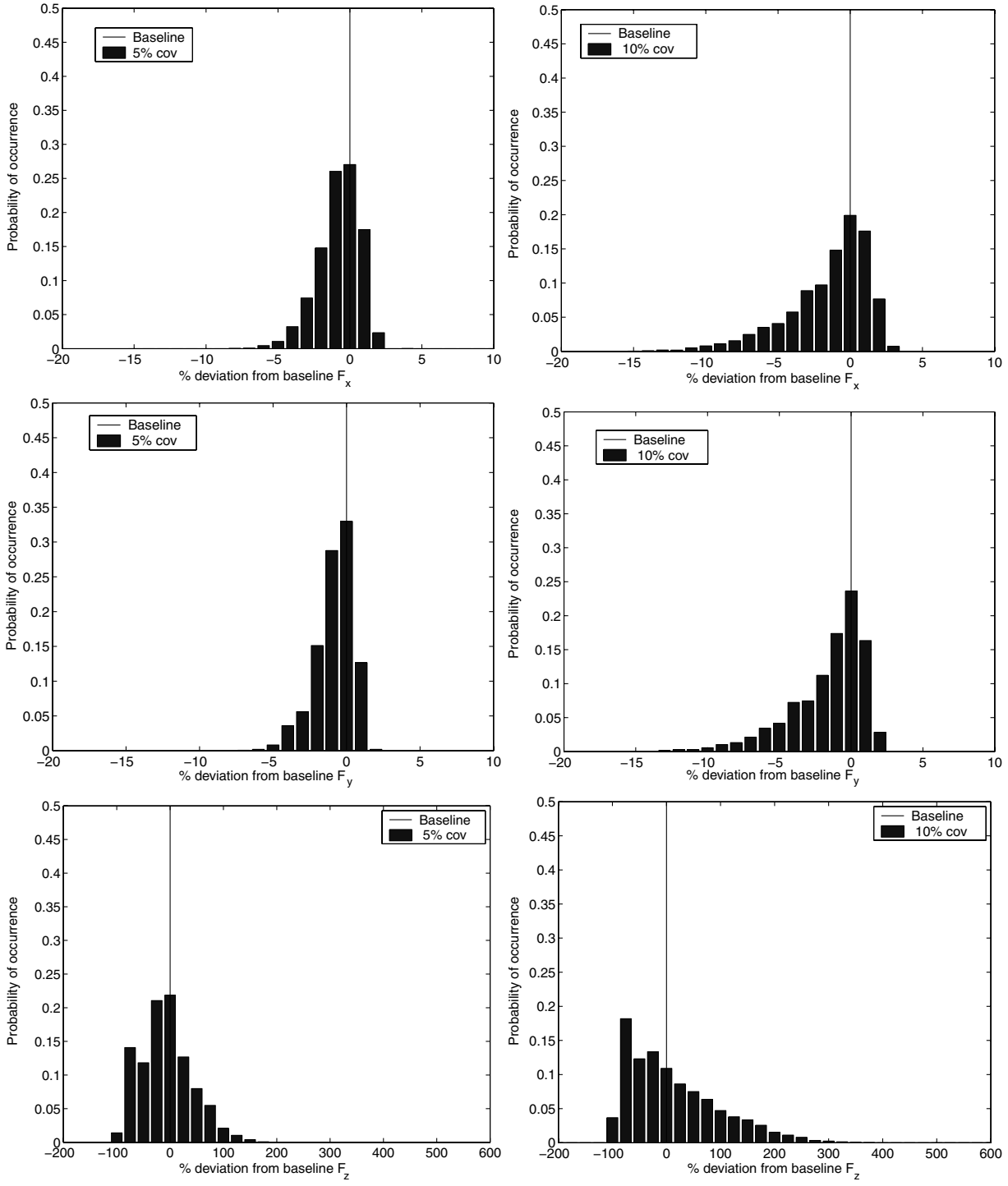

Fig. 14 Probability histograms of the hub vibratory forces.

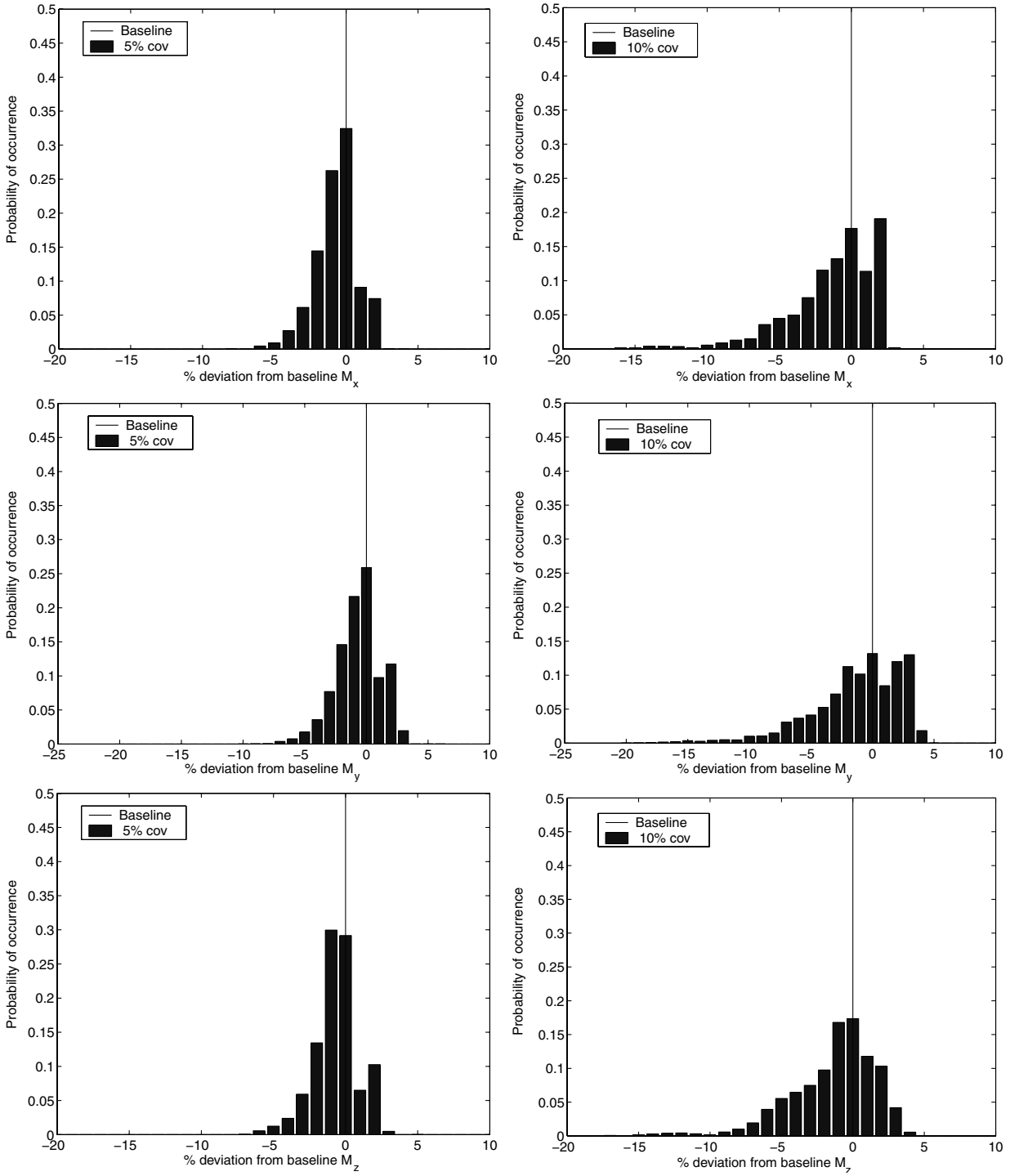

Fig. 15 Probability histograms of the hub vibratory moments.

stiffness, and centrifugal stiffness is unaltered. Therefore, the uncertainty impact on the rotating natural frequencies varies for each mode inversely with respect to the influence of centrifugal stiffness over the corresponding overall stiffness. For a hingeless rotor blade with uniform mass, the centrifugal stiffening has different impacts on the flap, lag, and torsional motions of the rotating blade [39]. The centrifugal stiffness dominates the flap motion of the rotating blade, compared with its structural stiffness. For the lag motion, the structural stiffness dominates the motion, compared with the centrifugal stiffness. Therefore, the effect of uncertainty in the structural stiffness has a greater influence on the lag frequencies than with the flap frequencies, as shown in Table 4. For the torsional motion, the structural stiffness is comparatively higher than the centrifugal stiffness and therefore the randomness in torsional stiffness has a higher impact on torsion rotating frequencies.

The stochastic rotating natural frequencies given in Fig. 6 show a probability of coinciding with the integer multiples of rotor speed [39]. From Fig. 6, it is observed that the integer multiples of rotor speed occur in frequency bands of first torsion, second torsion, and second lag modes. That is, the impact of material uncertainty can possibly lead to resonance conditions of rotor blade and the resulting high levels of vibration.

C. Aeroelastic Response

The material uncertainty effects on the aeroelastic response of the composite rotor blade is evaluated at an advance ratio of 0.3 with a

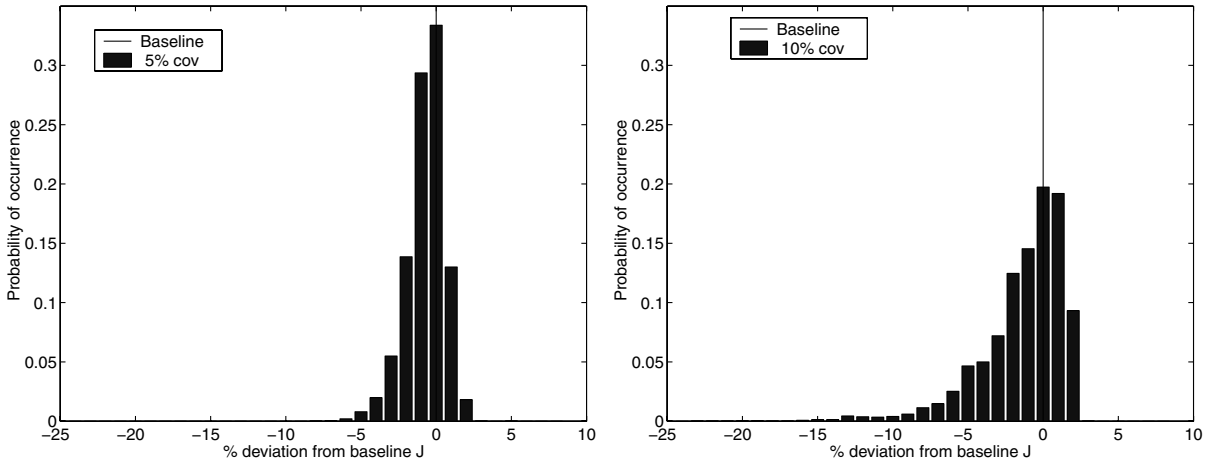

Fig. 16 Probability histograms of the vibration function.

rotorcraft aeroelastic analysis code [35]. The aeroelastic analysis is carried out for the 5000 cross-sectional stiffness matrices evaluated in Sec. IV.A.

The steady-state response of a helicopter blade rotating at speed Ω is periodic, with a period of 2π in a dimensionless timescale: $\psi = \Omega t$ [39]. The baseline and MCS of blade tip response for one revolution are shown in Figs. 9–11. The peak values of flap, lag, and torsion responses show substantial deviation from baseline predictions with respect to the material uncertainty. The scattering of the torsion response is higher in the region of azimuth value of 90 to 270 deg than in other regions. There is a change in the steady as well as the harmonic content of the response. The large impact of material uncertainty on torsion response is a very important observation because the elastic twist is critical not only for aeroelastic effects on the rotor blade, but also for the control of the helicopter as a whole.

D. Vibratory Hub Loads

In helicopters, the aerodynamic loads acting on the rotor blades are transmitted to the fuselage and cause severe vibrations. For a rotor with N blades, the loads with frequencies that are integer multiples of $N\Omega$ are transmitted from the rotor to the hub [39]. The prediction of these vibratory loads is a key issue in the aeroelastic analysis, design, and optimization of a rotorcraft [2]. Therefore, for a four-bladed rotor considered in this study, the impact of material uncertainty on these $4/\text{rev}$ vibratory loads (which are longitudinal shear F_x, lateral shear F_y, vertical shear F_z, rolling moment M_x, pitching moment M_y, and yawing moment M_z) are studied. The $4/\text{rev}$ forces are normalized by the rotor steady thrust, and the $4/\text{rev}$ moments are normalized by the rotor steady yawing moment.

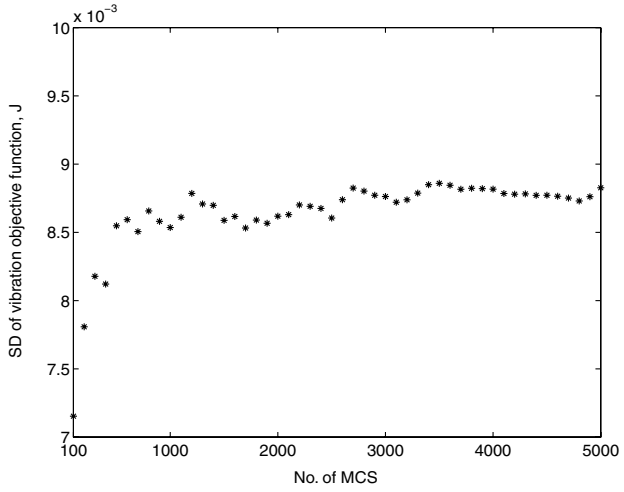

Fig. 17 Convergence of the vibration objective function.

The baseline and MCS of $4/\text{rev}$ vibratory forces and moments are shown in Figs. 12 and 13. The magnitudes of vibratory hub loads are given in Table 5. The deviation of mean, median, and extreme values from the baseline (deterministic) value varies for each component of the vibratory loads. The extreme values of vertical force show a deviation of -82 to 298% from its baseline value. The longitudinal and lateral forces show a deviation of -7 to 5% from their baseline value. The rolling and pitching moments show a scattering of around -9 to 7% from their baseline values. The vibratory yawing moment shows a scattering of around -7 to 16%. The probability histograms of $4/\text{rev}$ loads given in Figs. 14 and 15 show non-Gaussian-type distributions. The histograms for case II (i.e., for a COV of 10% in material properties) are also shown in Figs. 14 and 15. There is a proportional increase in spread of the histograms of vibratory hub loads due to the increase in material uncertainty. However, the shapes of the histograms remain similar. Note that both case I and case II MCS are run with 5000 points.

Most of the aeroelastic optimization studies for vibration reduction have the objective function as a scalar norm of the magnitudes of $4/\text{rev}$ forces and $4/\text{rev}$ moments, as given next [2]:

$$J = \sqrt{F_x^2 + F_y^2 + F_z^2} + \sqrt{M_x^2 + M_y^2 + M_z^2} \tag{7}$$

The uncertainty effect on the preceding vibration function J is shown in Fig. 16. The vibration function J shows a scattering of -7 to 4% from the baseline for case I, with a non-Gaussian distribution. For case II, the shape of the distribution remains quite similar, with most of the points to the left of the mean. However, the distribution spread is increased for case II. The preceding results clearly indicate that the randomness in composite material properties has a considerable influence on the vibratory-load predictions. The convergence of standard deviation of vibration function J is shown in Fig. 17. The stochastic aeroelastic analysis with 5000 MCS takes about 50 h of CPU time on a PC with a quad-core processor.

In the current work, the UMARC code is used for aeroelastic simulations. However, it will be interesting to compare the uncertainty-analysis results from different rotorcraft comprehensive analysis codes such as CAMRAD II and DYMORE in future work. Further, the aeroelastic analysis uses the classical Euler–Bernoulli model for the force-displacement relationship of the rotor blade. However, the Timoshenko model will increase the accuracy of third or higher bending frequencies and is a topic for further research.

V. Conclusions

The aeroelastic response of a composite helicopter rotor with material uncertainty is studied. Young's moduli and Poisson's ratios of the composite material are modeled as independent normally distributed random variables. The effect of material uncertainties on the cross-sectional stiffness, rotating natural frequencies, aeroelastic response, and vibratory hub loads of the composite rotor blade are

evaluated using Monte Carlo simulations. The following conclusions are drawn from this study for a COV of 5% in the material properties:

1) The flap, lag, and torsional stiffnesses of the composite rotor blade show COVs of 4.46, 4.21, and 3.94%, respectively. The extension-lag coupling shows a COV of 3.94%. The stiffnesses show normal distribution with a COV contraction, compared with the material properties.

2) The flap, lag, and torsional fundamental natural frequencies of the rotating composite blade show COVs of 0.21, 1.85, and 1.66%, respectively. The flap natural frequencies are less sensitive to material uncertainty, compared with the lag and torsional frequencies. The COVs of rotating natural frequencies vary with flap, lag, and torsion modes because of the varying relative importance of the corresponding structural stiffness vis-a-vis the centrifugal stiffness. However, the overall effect is that frequencies show a COV contraction relative to the material property COV, with the values ranging from 0.21 to 1.94% for the first two lag, three flap, and two torsion frequencies.

3) The stochastic rotating natural frequencies of the first and second torsion modes and second lag mode can coincide with integer multiples of the rotor speed. The finite probability for the occurrence of 4/rev frequency can lead to a resonance condition of the rotor blade and result in high vibration levels.

4) The aeroelastic response of the composite helicopter rotor shows a considerable deviation from its baseline value, due to material uncertainty. The probability distribution of the blade tip response varies along the azimuth because of the varying structural and aerodynamic interactions.

5) The 4/rev vibratory loads show considerable deviations from their corresponding deterministic values, due to material uncertainty. The histograms of vibratory loads show non-Gaussian distributions. The material uncertainty has a higher impact on the vibratory vertical force and somewhat less impact on the other vibratory loads. The 4/rev vertical hub load shows a deviation of −82 to 298% from the baseline value. The longitudinal and lateral forces show scattering of −7 to 5% from their baseline values. The extreme values of 4/rev rolling, pitching, and yawing moments show scattering of −9 to 16% from their own baselines. It is clear that aleatory uncertainty can play a major role in the reliability of prediction of vibratory loads from helicopter aeroelastic analysis.

6) The objective function used in aeroelastic optimization for vibration reduction shows a scattering of −7 to 4% from its baseline value with a non-Gaussian distribution. The use of this sum of scalar norm of forces and moments therefore contracts the aleatory uncertainty effects on vibration predictions.

The effect of doubling the COV of material properties from 5 to 10% proportionally increases the spread of the distributions of blade stiffness, frequencies, and vibratory hub loads. However, the nature of the distribution remains similar. The results of this study clearly show that the aeroelastic analysis, design, and optimization of rotorcraft should consider the randomness in composite material properties.

References

[1] Friedmann, P. P., "Rotary-Wing Aeroelasticity: Current Status and Future Trends," *AIAA Journal*, Vol. 42, No. 10, 2004, pp. 1953–1972. doi:10.2514/1.9022

[2] Ganguli, R., "A Survey of Recent Developments in Rotorcraft Design Optimization," *Journal of Aircraft*, Vol. 41, No. 3, 2004, pp. 493–510. doi:10.2514/1.58

[3] Ganguli, R., Chopra, I., and Weller, W. H., "Comparison of Calculated Vibratory Rotor Hub Loads with Experimental Data," *Journal of the American Helicopter Society*, Vol. 43, No. 4, 1998, pp. 312–318.

[4] Datta, A., and Chopra, I., "Validation and Understanding of UH-60 Vibratory Loads in Steady Level Flight," *Journal of the American Helicopter Society*, Vol. 49, No. 3, 2004, pp. 271–287.

[5] Pettit, C. L., "Uncertainty Quantification in Aeroelasticity: Recent Results and Research Challenges," *Journal of Aircraft*, Vol. 41, No. 5, 2004, pp. 1217–1229. doi:10.2514/1.3961

[6] Mavris, D. N., Bandte, O., and DeLaurentis, D. A., "Robust Design Simulation: A Probabilistic Approach to Multidisciplinary Design," *Journal of Aircraft*, Vol. 36, No. 1, 1999, pp. 298–307.

[7] Poirion, F., "On some Stochastic Methods Applied to Aeroservoelasticity," *Aerospace Science and Technology*, Vol. 4, No. 3, 2000, pp. 201–214. doi:10.1016/S1270-9638(00)00118-8

[8] Lindsley, N. J., Beran, P. S., and Pettit, C. L., "Effects of Uncertainty on Nonlinear Plate Aeroelastic Response," 43rd AIAA/ASME/ASCE/AHS/ASC Structures, Structural Dynamics, and Materials Conference, Denver, CO, AIAA Paper 2002-1271, Apr. 2002.

[9] Pettit, C. L., and Grandhi, R. V., "Optimization of a Wing Structure for Gust Response and Aileron Effectiveness," *Journal of Aircraft*, Vol. 40, No. 6, 2003, pp. 1185–1191.

[10] Attar, P. J., and Dowell, E. H., "Stochastic Analysis of a Nonlinear Aeroelastic Model Using the Response Surface Method," *Journal of Aircraft*, Vol. 43, No. 4, 2006, pp. 1044–1052. doi:10.2514/1.17525

[11] Murugan, S., Ganguli, R., and Harursampath, D., "Aeroelastic Response of Composite Helicopter Rotor with Random Material Properties,"*Journal of Aircraft*, Vol. 45, No. 1, 2008, pp. 306–322. doi:10.2514/1.30180

[12] Oberkampf, W. L., and Helton, J. C., "Mathematical Representation of Uncertainty," 42nd AIAA/ASME/ASCE/AHS/ASC Structures, Structural Dynamics, and Materials Conference, Seattle, WA, AIAA Paper 2001-1645, Apr. 2001.

[13] Cheng, J., Jiang, J. J., and Xiao, R. C., "Aerostatic Stability Analysis of Suspension Bridges Under Parametric Uncertainty," *Engineering Structures*, Vol. 25, No. 13, 2003, pp. 1675–1684. doi:10.1016/S0141-0296(03)00146-9

[14] Kareem, A., "Aerodynamic Response of Structures with Parametric Uncertainties," *Structural Safety*, Vol. 5, No. 3, 1988, pp. 205–225. doi:10.1016/0167-4730(88)90010-0

[15] Onkar, A. K., Upadhyay, C. S., and Yadav, D., " Stochastic Finite Element Buckling Analysis of Laminated Plates with Circular Cutout Under Uniaxial Compression," *Journal of Applied Mechanics*, Vol. 74, No. 4, 2007, pp. 798–809. doi:10.1115/1.2711230

[16] Babuka, I., Andersson, B., Smith, P. J., and Levin, K., "Damage Analysis of Fiber Composites Part I: Statistical Analysis on Fiber Scale," *Computer Methods in Applied Mechanics and Engineering*, Vol. 172, Nos. 1–4, 1999, pp. 27–77. doi:10.1016/S0045-7825(98)00225-4

[17] Singh, B. N., Yadav, D., and Iyengar, N. G. R., "Free Vibration of Composite Cylindrical Panels with Random Material Properties," *Composite Structures*, Vol. 58, No. 4, 2002, pp. 435–442. doi:10.1016/S0263-8223(02)00133-2

[18] Onkar, A. K., and Yadav, D., "Non-Linear Response Statistics of Composite Laminates with Random Material Properties Under Random Loading," *Composite Structures*, Vol. 60, No. 4, 2003, pp. 375–383. doi:10.1016/S0263-8223(03)00049-7

[19] Venter, G., and Haftka, R. T., "Response Surface Approximations for Cost Optimization of Dropped Ply Composite Laminates with Uncertainty," *7th AIAA/USAF/NASA/ISSMO Symposium on Multidisciplinary Analysis and Optimization*, AIAA, Reston, VA, 1998, pp. 1145–1163.

[20] Kapania, R. K., and Goyal, V. K., "Free Vibration of Unsymmetrically Laminated Beams Having Uncertain Ply Orientations," *AIAA Journal*, Vol. 40, No. 11, 2002, pp. 2336–2344.

[21] Smith, E. C., and Chopra, I., "Aeroelastic Response, Loads, and Stability of a Composite Rotor in Forward Flight," *AIAA Journal*, Vol. 31, No. 7, 1993, pp. 1265–1273. doi:10.2514/3.49066

[22] Ganguli, R., and Chopra, I., "Aeroelastic Optimization of a Helicopter Rotor with Two-Cell Composite Blades," *AIAA Journal*, Vol. 34, No. 4, 1996, pp. 835–841. doi:10.2514/3.13147

[23] Jung, S. N., and Park, I. J., "Structural Behavior of Thin- and Thick-Walled Composite Blades with Multicell Sections," *AIAA Journal*, Vol. 43, No. 3, 2005, pp. 572–581. doi:10.2514/1.12864

[24] Murugan, M. S., and Ganguli, R., "Aeroelastic Stability Enhancement and Vibration Suppression in a Composite Helicopter Rotor," *Journal of Aircraft*, Vol. 42, No. 4, 2005, pp. 1013–1024. doi:10.2514/1.5652

[25] Cesnik, C. E. S., and Hodges, D. H., "VABS: A New Concept for Composite Rotor Blade Cross-Sectional Modeling," *Journal of the American Helicopter Society*, Vol. 42, No. 1, 1997, pp. 27–38.

[26] Yu, W., Volovoi, V. V., and Hodges, D. H., "Validation of the

Variational Asymptotic Beam Sectional Analysis," *AIAA Journal*, Vol. 40, No. 10, 2002, pp. 2105–2112.

[27] Elishakoff, I., *Probabilistic Methods in the Theory of Structures*, Wiley, New York, 1983.

[28] Kleiber, M., and Hien, T. D., *The Stochastic Finite Element Method, Basic Perturbation Technique and Computer Implementation*, Wiley, New York, 1992.

[29] Lutes, L. D., and Sarkani, S., *Stochastic Analysis of Structural and Mechanical Vibrations*, Prentice–Hall, Upper Saddle River, NJ, 1997.

[30] Choi, S., Grandhi, R. V., and Canfield, R. A., *Reliability-Based Structural Design*, Springer–Verlag, London, 2006.

[31] Haldar, A., and Mahadevan, S., *Reliability Assessment Using Stochastic Finite Element Analysis*, Wiley, New York, 2000.

[32] Choi, S. K., Grandhi, R. V., Canfield, Robert, A., and Pettit, C. L., "Polynomial Chaos Expansion with Latin Hypercube Sampling for Estimating Response Variability," *AIAA Journal*, Vol. 42, No. 6, 2004, pp. 1191–1198.
doi:10.2514/1.2220

[33] Bae, H. R., Grandhi, R. V., and Canfield, R. A., "Uncertainty Quantification of Structural Response Using Evidence Theory," *AIAA Journal*, Vol. 41, No. 10, 2003, pp. 2062–2068.

[34] Kunz, D., "Comprehensive Rotorcraft Analysis: Past, Present, and Future," 46th AIAA/ASME/ASCE/AHS/ASC Structures, Structural Dynamics and Materials Conference, Austin, TX, AIAA Paper 2005-2244, Apr. 2005.

[35] Bir, G., and Chopra, I., "University of Maryland Advanced Rotorcraft Code (UMARC) Theory Manual," Univ. of Maryland Rept. 92-02, College Park, MD, 1992.

[36] Smith, E. C., "Vibration and Flutter of Stiff In-Plane Elastically Tailored Composite Rotor Blades," *Mathematical and Computer Modelling*, Vol. 19, Nos. 3–4, 1994, pp. 27–45.
doi:10.1016/0895-7177(94)90055-8

[37] Barwey, D., and Peters, D. A., "Optimization of Composite Rotor Blades with Advanced Structural and Aerodynamic Modeling," *Mathematical and Computer Modelling*, Vol. 19, Nos. 3–4, 1994, pp. 193–219.
doi:10.1016/0895-7177(94)90064-7

[38] Yu, W., "Variational Asymptotic Modeling of Composite Dimensionally Reducible Structures," Ph.D. Dissertation, Georgia Inst. of Technology, Atlanta, 2002.

[39] Johnson, W., *Helicopter Theory*, Princeton Univ. Press, Princeton, NJ, 1980.

F. Pai
Associate Editor